

# Cavities in Mass-Impregnated HVDC Subsea Cables Studied by AC Partial Discharge Measurements

M. Runde, O. Kvien, H. Förster and N. Magnusson

SINTEF Energy Research,  
NO-7465 Trondheim, Norway

## ABSTRACT

Partial discharge measurements have been used for studying shrinkage voids in the insulation of mass-impregnated high voltage DC subsea power cables. Three 4.5-m long cable samples were subjected to ac partial discharge measurements at different ambient temperatures, both under isothermal conditions and after load current turn-offs. Two distinctly different phase resolved partial discharge patterns were observed, suggesting that two different "types" of cavities were created. The type causing by far the most powerful discharges appeared a few hours into the cooling period after load turn-off, which coincides in time with when load cycling breakdowns during type testing usually occur. Current loading has a significant effect on the cavities, as it leaves them – at least temporary – with a different dielectric strength afterwards. The mechanisms behind this change are not identified, but the associated time constants are of the order of days and weeks. Consequently, accurately determining the limitations of such cables with regard to their ability to withstand polarity reversals and rapid load changes may be more complicated than previously assumed.

Index Terms — high voltage techniques, HVDC transmission, partial discharges, power cable insulation

## 1 INTRODUCTION

**HIGH** voltage direct current (HVDC) submarine power cables [1] are becoming an increasingly important part of power transmission systems as they interconnect land-based ac systems separated by long sea crossings. This development is particularly apparent in Europe, where existing and future HVDC subsea links both in the Mediterranean and in the North Sea facilitate electric power exchange with continental Europe.

The so-called mass-impregnated non-draining (MIND) cable has up to now been the technology of choice for these links. The electrical insulation here consists of lapped Kraft paper impregnated with high-viscosity oil (the "mass"). For cables of the highest voltage ratings some 200 layers of paper tapes, each around 0.1 mm thick and 20–30 mm wide are lapped into a thickness of around 20 mm. The paper tapes are wound with a pitch that exceeds the tape width somewhat, so that a few millimeters wide helical butt gaps are formed in each layer. This makes it possible to bend the cable without damaging the paper tapes. After the impregnation the butt gaps are assumed to be filled with mass. A lead sheath permanently seals off the insulation system and prevents water ingress.

Subsea HVDC MIND cables are an old, resilient and well-proven technology with an excellent service record. Most of the failures that have occurred have been caused by external factors

such as trawl doors and anchors.

The operational patterns for typical HVDC links have in recent years been gradually changing. Market demands now call for larger and faster load changes than in the past. This is likely to impose more severe stresses on the insulation system of the cables. In particular, polarity reversals and the cooling period after a load reduction or turn-off are assumed to be critical. The mass has a thermal expansion coefficient around ten times higher than the paper [2]. As the insulation cools after a load turn-off, the pressure in the insulation falls. The temperature reduction and the accompanying thermal contraction are larger near the conductor than at the outer parts of the insulation. Migration of mass through the paper layers is slow, so it is assumed that voids or cavities may form as the contracting, high-viscosity mass is not able to fill the available volume.

A special type of dielectric breakdown observed in the cooling phase of the load cycling part of the type test [3, 4] is assumed to be caused by such shrinkage cavities. The first voids are probably formed in the volume of the butt gaps, before they expand and extend axially between the paper layers to the butt gaps of the next layer. A path along the cable axis with significantly lower dielectric strength is thus created. Partial discharges (PDs) ignite, and eventually this develops into a breakdown channel. Subsequent dissections have revealed carbonized channels extending more than a meter along the axis of the cable [5, 6].

This phenomenon, referred to as a load-cycling breakdown, is believed to be among the limiting factors with regard to dynamic loading of MIND cables (although it has mainly been experienced

---

*Manuscript received on 8 October 2018, in final form 15 December 2018, accepted xx Month 20yy. Corresponding author: M. Runde.*

during type testing). However, beyond the simple and partly speculative descriptions above, not much is known about how this process initiates and develops, and – more importantly – what the decisive contributing factors are. Pressure and pressure gradients in the insulation under the transient conditions of a load change obviously play a role, but how these influences on the number, size, shape, location, internal gas pressure and dielectric properties of the shrinkage voids has not been clarified in any detail.

Most of the published work addressing this phenomenon has applied either small-scale experiments, numerical modelling or PD measurements. Evenset [7] has studied the formation of cavities in an idealized setup consisting of a small glass tube filled with mass and a paper strip. It appeared that the nucleation site for the cavities was at the paper surface and that a considerable quasi-static tensile stress in the mass, corresponding to around 9 bar, was required before cavities were created. He also made a planar arrangement where four mass-impregnated paper sheets with slits simulating butt gaps were placed between rigid glass plates and cooled down [8]. Usually, the first void appeared in the butt gap.

Numerical simulations of the internal pressure in MIND cables have indicated that both very low (vacuum) and high pressures (>10 bar) can be expected during load cycling [2, 9]. Low pressures are consistent with shrinkage void formation, whereas large radial pressure differences may cause a radial flow of mass and thereby change the cavity distribution [10].

Recently, models including thermo-mechanical calculations of the internal pressure, and how this is affected by external pressure and by cable loading, have been developed [11, 12].

Several studies that include PD measurements after a load turn-off of several tens of meters long MIND cables have been published [2, 5, 13, 14]. The PD activity, typically measured as the repetition rate for PDs over a certain magnitude, starts immediately after the turn-off, has a maximum 1–5 hours into the cooling period, and then gradually declines. This behavior is attributed to void formation as described above, and that the electrical conductivity of the mass becomes lower as temperature drops.

The investigations reported on here used PD measurements to experimentally study and characterize voids and void formation in MIND cable insulation. In contrast to the works referred to above, ac and not DC voltage was applied. This approach is new and has a couple of important advantages. First, meaningful investigations can be carried out by applying rather modest voltages; in the present case ac voltages up to 90 kV were used to study cavities in MIND cables rated for around 500 kV DC. This significantly reduces the cost and complexity of the measurements, including the preparation of suitable cable terminations.

Second, equipment for recording, presenting, statistical analysis and interpretation of PDs obtained under ac is well developed and commercially available. Sophisticated techniques such as phase resolved partial discharge (PRPD) analysis being used here, have become widely used tools for identifying and characterizing the PD sources.

## **2 PD MEASUREMENTS ON MIND CABLE SUBJECTED TO AC**

### **2.1 CONCEPT**

Fully mass-impregnated paper insulation has a formidable dielectric strength. If voids or crevices are created, or paper layers delaminate, this in most cases results in a local reduction of the

dielectric strength, and – depending on the applied voltage – PDs may ignite.

PD measurements under ac voltages of different magnitudes and under various ambient temperatures and loading conditions have been carried out. The recorded data (PD inception and extinction voltages, and PRPD plots) are used to obtain information about the creation and behavior of cavities in the insulation. Generally, a low inception voltage, and many and large PDs signify that many and large voids exist. Larger PDs are the more interesting ones in the present context, as these are believed to be generated by cavities that are potentially more harmful to the integrity of the insulation system of a MIND cable than small ones.

It should be emphasized that PD measurements under ac here are used as a tool; this work does not concern the effects PDs may have on the insulation system under DC operation.

### **2.2 CABLE SAMPLES AND TERMINATIONS**

The test objects were three 4.5 m long sections of MIND cables from different manufacturers. Their voltage ratings are in the range 450–525 kV DC, and the lapped mass-impregnated paper insulation is 19–20 mm thick. Two of the samples – referred to as A and B – were taken from several kilometer-long spare cables, whereas the third – sample C – was cut from a few hundred meters long section of a cable that has been in service for several years. The cable lengths from where the samples were cut, have had their ends carefully sealed off to prevent air or mass from leaking into or out of the insulation.

When attempting to imitate the behavior of a (for all practical purposes) infinitely long cable in service by using short samples in a laboratory setup, the terminations of the test objects are critical parts. First, they need to be tight and able to withstand significant pressures. If air or mass is pressed out of or sucked into the insulation from or through the terminations, the laboratory setup no longer replicates true service conditions.

Second, thermal expansion may also cause the entire lapped insulation to slide axially relative to the conductor if the terminations are poorly designed. A sturdy mechanical fixture that prevents such relative movements is required.

Third, the terminations should not contain voids, sharp edges or other sources for PDs, neither external nor internal. Excessive PD activity from the cable ends may obscure the recordings from the cable itself.

When assembling a termination, the lead sheath and all the other protective layers of the cable must be removed, leaving the cable insulation – typically at a pressure somewhat below atmospheric – exposed to the ambient air. Thus, some air was inevitably entering in or was dissolved in the outer layers of the mass-impregnated paper. The problem was reduced by limiting the time the insulation was open to a minimum. Notwithstanding, the mass-impregnated paper insulation remains an integral part of the termination, and some PD activity is to be expected also from this part of the test object.

Figure 1 shows a cross-sectional drawing and a photo of the cable termination being developed and applied in the present investigations.

The brass connector at the end was firmly fastened to the cable conductor with five steel bolts (not shown in Figure 1a). It provided a low-resistance access to the conductor when passing current and averted axial movement of the insulation. The mastic filled up any open volumes between the mass-

impregnated paper and the brass connector.

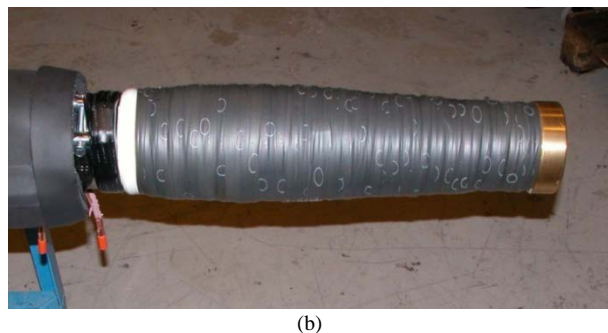
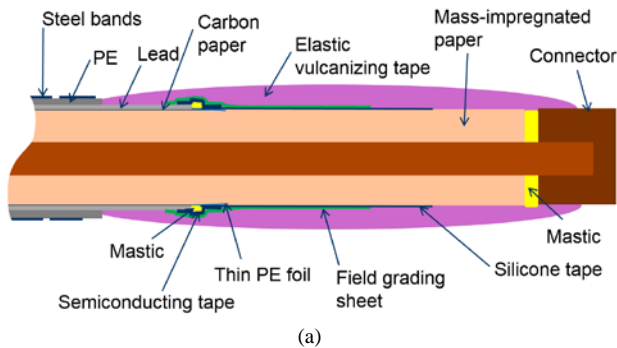


**Figure 1.** (a) Schematic cross-sectional drawing, and (b) photograph of the cable termination. The length is around 50 cm.

Concerning the electrical stresses, the most critical area is at the end of the carbon paper layer. The field grading sheet or pad causes the electric field here to be reduced and spread out over a longer portion of the insulation. The impregnation mass is chemically incompatible with the field grading materials, so thin polyethylene and silicone tapes were used to avoid direct contact. The outer layer of lapped elastic vulcanizing tape strongly compresses the entire assembly so that the internal pressure in the termination is probably higher than in the cable, at least at low temperatures. The vulcanizing tape is also a good electrical insulator. The steel bands and the galvanized steel armor wires of the MIND cable were firmly secured with a rugged hose clamp (barely visible in Figure 1 b).

This in-house termination design worked well for voltages up to approximately 100 kV ac. Compared to using the type of cable terminations installed on such cables when in normal HVDC operation, this turned out to be a compact, low-cost alternative, well-suited for the current purpose.

The ambient temperature of the cables, excluding the terminations, was controlled by using a heating/cooling machine that circulated a liquid in copper pipes wound onto the cable surface. The pipes were embedded in an around 5-cm thick layer of a flexible polymer compound filled with aluminum powder to increase its thermal conductivity, see Figure 2. This arrangement exerts no external pressure on the test object. Afterwards, sheets of polymer foam were wrapped on the outside to thermally insulate the test object from the laboratory ambient. The end of the copper pipes and the thermal insulation are visible to the left in Figure 1b.



**Figure 2.** Embedding the copper pipes in a thermally well-conducting compound to provide a good temperature control of the cable surface.

This setup made it possible to control the ambient temperature of the cable in the range  $-5$  to  $+40$  °C, even under rated load current.

### 2.3 SETUP FOR PD MEASUREMENTS

Two parallel systems for obtaining PD signals were applied, see Figure 3. A standard analogue setup consisting of 0.8 nF coupling capacitors and commercial PD shunts (Omicron CPL 542) was hooked up to both ends of the MIND cable. A common signal ground point was established on the lead sheath at the midpoint of the cable. The two signals were transmitted by coaxial cables of equal length to a 2.5 GS/s oscilloscope (Tectronix DPO 405-4). By comparing the arrival times of the same PD pulse, the approximate location (roughly within one meter) of its source could be determined.

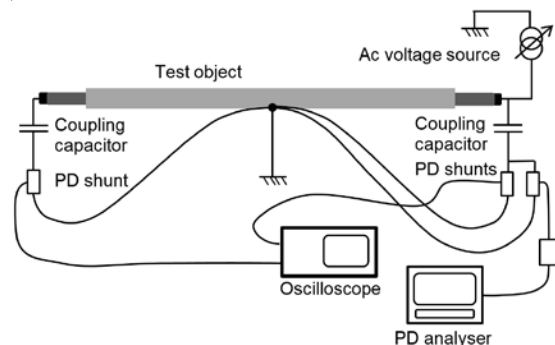


**Figure 3.** The PD measurement setup.

The other system was a commercial solution (Omicron MPD 600) comprising the same type of measuring shunt, a PD acquisition unit and a laptop computer with a software package for control, communication, presentation and storage of the obtained signals. The center frequency and width were set to 5 and 1 MHz, respectively, as this gave a decent signal-to-noise ratio. Dead time was set to 2  $\mu$ s. The measuring range was 5–10,000 units.

The amplitude of the PDs could not be properly calibrated as the PD signal was integrated and digitized, and the applied frequencies were far higher than used for IEC 60270 compliant PD measurements [15, 17]. By inserting a 100-pC signal from a PD calibrator at one of the cable terminations, a peak value of 30 units was measured. This indicates that the recordings cover PDs with apparent discharges ranging from approximately 15 to 30,000 pC. The PD activity over a certain recording period was visualized by displaying the amplitude and phase location of each recorded discharge by a dot, in so-called PRPD plots.

PRPD plots have become a commonly applied tool for describing and visualizing PDs in electrical insulation systems [15]. PDs from different defects, such as a needle electrode in gas, a cavity in a solid, a surface contamination, etc., have different polarity dependency, phase location and amplitude. Hence, the source type can usually be identified from the obtained PRPD plots.

### 3 RESULTS AND DISCUSSION

#### 3.1 TIME DOMAIN PLOTS

Figure 4 shows an oscilloscope screen dump with typical PD patterns covering a full 50-Hz cycle. The PDs come as bursts on the rising flank starting roughly a millisecond after voltage zero crossing. Almost no discharges appear on the declining flank.

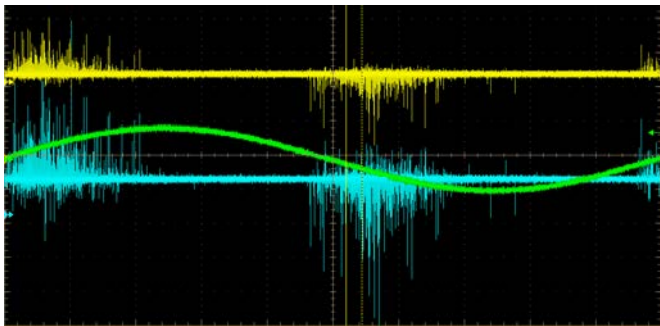


**Figure 4.** Typical PD patterns simultaneously recorded over a 20-ms interval in two channels. The applied voltage (sinusoidal curve) is 20 kV. The upper channel is from the cable end with two PD shunts, giving a 50% reduction in signal amplitude compared to the lower channel signal obtained at the other end.

Such a PD pattern is normally recognized as being generated by local dielectric breakdowns inside gas-filled voids in electrical insulation. Above a certain voltage, similar recordings were obtained on all three samples, and this is taken as evidence of that cavities existed in the cables.

As pointed out above, the fast, dual channel measurement facilitated a rough localization of a PD's source. Figure 5 shows the fronts of two PD signals acquired at the cable ends. Each plot covers 220 ns. The PD signals in the left image arrived at the oscilloscope approximately at the same time, indicating that the source was at the mid-section of the cable. In the right plot the upper channel signal is lagging the lower signal by around 17 ns. The signal propagation velocity  $v$  can be determined to 160 m/ $\mu$ s by  $v = c \sqrt{\mu_r/\epsilon_r}$  when assuming that  $\epsilon_r = 3.5$  and  $\mu_r = 1$  for MIND cable insulation. Thus, this delay indicates that the void where this PD occurred was located around a meter from the cable end where the lower signal was acquired.

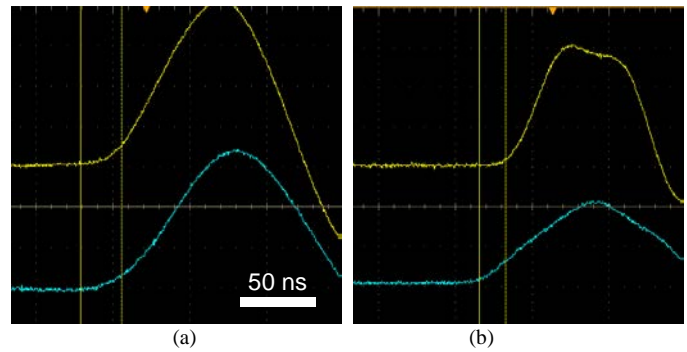


**Figure 5.** Oscilloscope screen dump of simultaneous dual channel recording of the front of PDs signal coming from the mid-section of the cable (a) and nearer to the end (b).

This investigation concerns PDs in the MIND cable insulation, so excessive PD activity in the terminations was unwanted and a potential source or error. By checking the location of the PDs as demonstrated in Figure 5, it was ensured that the PRPD plots and the recorded inception and extinction voltages reported on here were based on PDs from the cable itself, and not severely disturbed by flaws and irregularities in the terminations. This "quality assurance" was carried out as frequent visual oscilloscope inspections; no automatic signal gating or filtering was employed. A few measurement series were found to contain an excessively large fraction of PDs coming from one of the terminations. These results were simply discarded.

#### 3.2 PD INCEPTION AND EXTINCTION VOLTAGES

Figure 6 shows PD inception and extinction voltages obtained as a function of temperature for the three objects examined. The cables were unloaded, i.e., at isothermal condition, and the temperature was not monotonously decreased or increased, but moved up and down between different setpoints in an arbitrary manner. The cables were left to rest at the setpoint temperature for at least 24 h before the measurements started. The voltage was increased at a rate of 20 kV/min until PDs were detected, and then lowered with the same rate until they disappeared.

For samples A and B one series of measurements was carried out on each, whereas object C was subjected to several series, also including measurements after a rated load current had been passed at an elevated ambient temperature. Each series was typically completed within a week's time, and the time elapsed between two series was around a month. In this period cable C rested at room temperature.

The general observation is that inception and extinction voltages increase with increasing temperature for all cables. For the virgin objects, cable A and B, no PDs were observed at temperatures above 12 and 14 °C, respectively. Several tests above these temperatures, and with applying up to 70 kV, were run on these samples, but no PDs could be detected. When only considering the results obtained before load current was passed, sample C did not become "silent" when using this PD measuring setup until the temperature exceeded 25 °C.

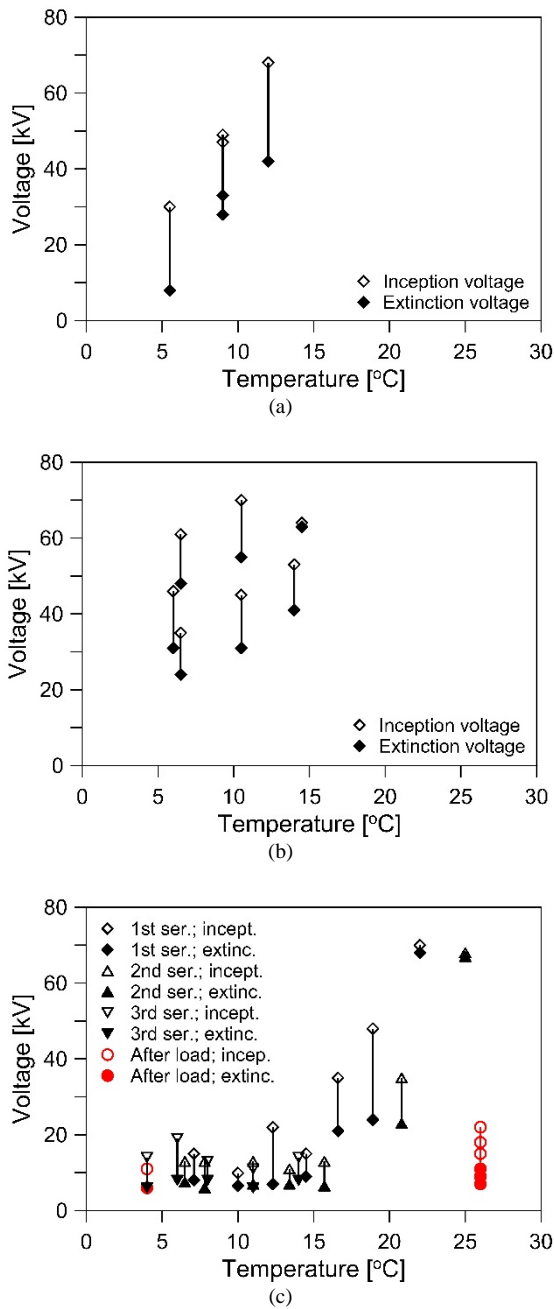


**Figure 6.** PD inception and extinction voltages under isothermal conditions for cable samples A (a), B (b) and C (c). Lines connect the inception and extinction voltage recordings for a given test to display this voltage span.

The obvious interpretation is that the observed temperature dependency of the PD activity is related to thermal contraction of the mass. Below a certain temperature, cavities of a size and capacitance sufficient to produce PDs large enough to be picked up by the recording system are formed. When further decreasing the temperature, the cavities increase in number and/or size and the inception and extinction voltages become lower.

Sample C differs from A and B in that it – among other things – earlier has been in normal service and thus has carried load currents. Whether the previous current loading is the reason for the PDs in the first three series appearing at somewhat higher

temperatures than in objects A and B cannot be established.

Current loading during the present test campaign did however, profoundly change the PD behavior of sample C. Rated load current was applied for one day, and since no forced cooling was applied, the surface temperature of the cable reached 35 °C. Measurements obtained under isothermal conditions at 26 °C the following week revealed PDs at voltages as low as 6 kV, see the circle symbols in Figure 6c. Before passing current, voltages above some 70 kV were needed to ignite PDs at this temperature.

One month later, a fifth PD measurement series on sample C was initiated, also at room temperature. It was now found that no PDs ignited, even when applying 80 kV several times during the week. Hence, in terms of its PD behavior, the cable now appears to be closer to what it was prior to the one-day current loading, i.e., again with ignition voltages near or above the upper measuring range of 80 kV. Consequently, the change imposed by the load current and accompanying temperature rise that reduced the ignition voltage to some 15–20 kV was of a temporary nature, lasting for somewhere between a week and a month.

The thermal time constant of the cable in the current setup is approximately half a day, so this behavior cannot be attributed to thermal contraction and expansion alone. Clearly, there are other, slower processes at work in the insulation system when and after the cable carries current. For example, if gas dissolved in the mass is slowly released into freshly created cavities and increases their internal gas pressure, Paschen's law states that this greatly influences the dielectric strength and thus presumably also on PD inception and extinction voltages. A radial flow of mass caused by the pressure gradient in the insulation, or simply many smaller cavities gradually combining into fewer larger ones, are also likely to change the PD behavior.

### 3.3 PD CHARACTERISTICS AT ISOTHERMAL CONDITIONS

After determining the inception voltages, the amplitude and phase location for all detected PDs were recorded over a 5-min period at constant voltages, typically 20, 40, 60 and 70 kV. The PD number and amplitude were in general found to increase with increasing voltage and with decreasing temperature for all three cable samples. This is consistent with that the number or size of the cavities in the insulation increase as temperature drops and the mass contracts more than the paper.

When presenting these measurements as PRPD plots, two clearly distinct patterns – occasionally superimposed – emerge. Figure 7 shows three examples. The phase location and amplitude of each PD is displayed by a dot. Amplitudes are displayed on a logarithmic scale on the vertical axis covering more than three decades. When many PDs with the same phase location and amplitude are collected, this is indicated by a more intense color.

The upper plot is a typical example of a PRPD plot that in the literature is commonly referred to as a "rabbit-like" pattern [17, 18]. Both half cycles are the same, with a large portion of the PDs around the zero crossing, i.e., when the derivative of the voltage is at its maximum. The magnitude of these PDs never exceeded 100 units.

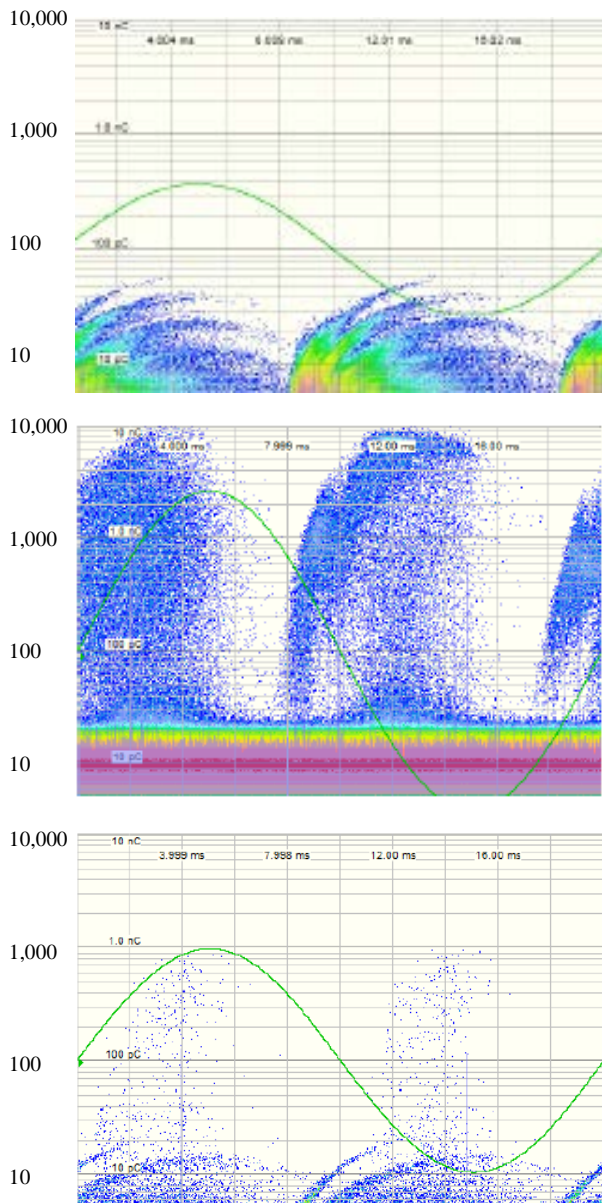


**Figure 7.** Typical examples of PRPD plots obtained from the three cable samples. The upper one is a typical example of "rabbit-like" shape; the middle is clearly different with much larger amplitudes, whereas the lower shows both features. These plots were acquired from cable sample A, B and A, respectively. (The measurements are not properly calibrated, so the vertical axis scaling is not correct. The red and yellow bands below 20 units in the middle plot are amplifier noise and should be ignored.)

The middle plot contains PDs with amplitudes more than two orders of magnitude larger than seen in the "rabbit-like" pattern. This pattern is also the same for both polarities. If using a linear scale on the vertical axis, this pattern may resemble what is referred to as a "triangle" PRPD pattern [17].

The standard interpretation of both the "rabbit-like" and "triangle" patterns is that the sources are cavities in the insulation. The quite distinct differences between the two may suggest that they originate in different types of cavities. It can be speculated that the "rabbit-like" is caused by many and small cavities located in the mass volume of the butt gaps, as the PDs

appear in large numbers, their amplitudes are small and presumably just a small portion of them exceed the lower limit of the measuring range of 5 units.

The other pattern with much greater amplitudes, sometimes exceeding the 10,000 units as in the middle plot of Figure 7, may be generated by a source with a much higher capacitance. Cavities or cracks formed by "delamination" of paper layers or by expansion/wedging from butt gaps and in between paper layers may be such a source. This cavity geometry is associated with large surfaces and much greater capacitances and charges than for example a small spherical cavity in the mass volume of a butt gap. The energy released by a PD thus becomes considerably larger.

### 3.4 PRPD PATTERNS AFTER LOAD TURN-OFFS

PD measurements were also carried out after current turn-offs on cable samples A and B and at various ambient temperatures (3, 6 and 13 °C). The procedure was as follows: First, the cable was cooled for a day to attain isothermal conditions. Then DC current was passed for a day such that the radial heat flow from the conductor and the accompanying temperature gradient in the insulation reached steady state. The current was then switched off, the current leads disconnected, PD measurement equipment hooked up, and high voltage ac was applied, all within a minute's time. Hence, the first PRPD plot could be completed some six minutes after load turn-off. More plots were recorded at increasing time intervals during the next 24 h. The voltage was turned off between the measurements.

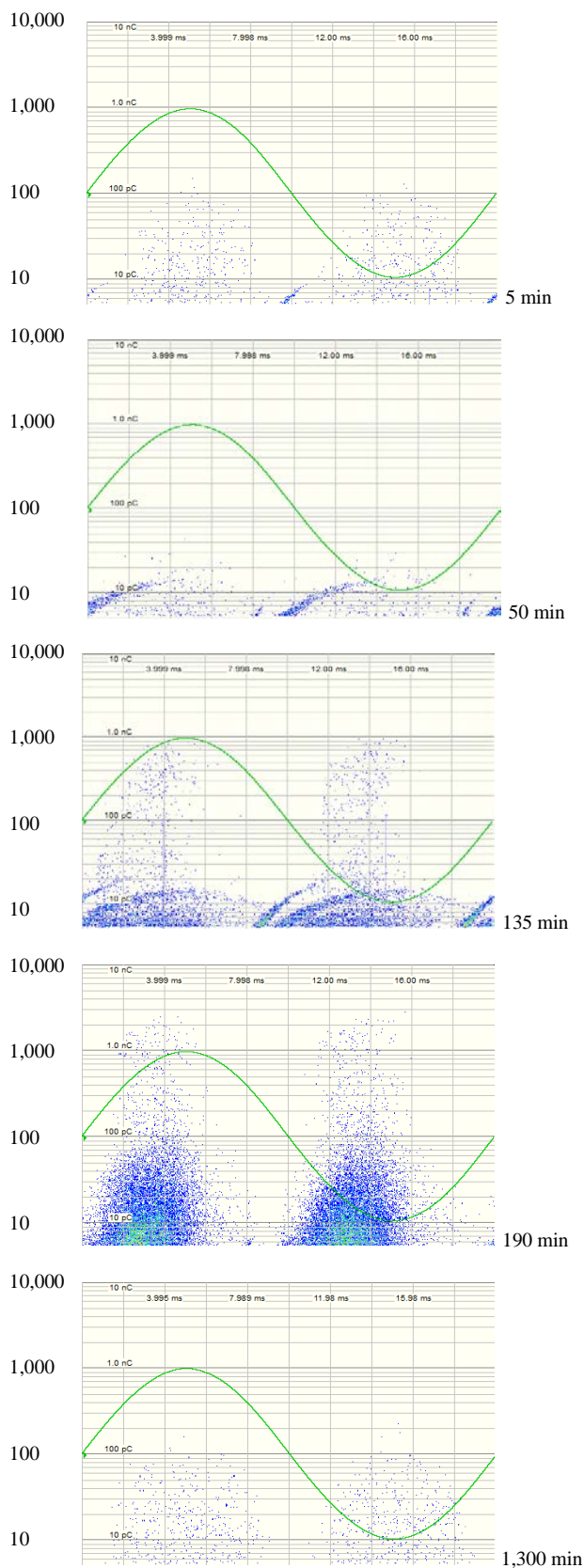
Immediately after current turn-off all cables were quiet, i.e., without observable PDs, even at 70 kV. After a few minutes, PDs forming "rabbit-like" PRPD patterns start appearing. Their repetition rate increased steadily and reached a maximum 1–3 h into the cooling period. About at the same time the other, more powerful type of PDs starts appearing. They gradually increase in magnitude and frequency, for later to slowly fade out. Towards the end of the 24 h recording period both types of PDs either have become far less intense or died out completely.

Figure 8 shows PRPD plots obtained from one of the load turn-off tests, illustrating this narrative.

At stationary conditions and with rated load current, the temperature drop across the insulation layer of the cables is around 12 °C, and an additional couple of degrees to the outer surface of the cable. Hence, immediately after load turn-off the temperature at the innermost layers of the insulation was around 17, 20 and 27 °C in these tests. The lack of PDs immediately after load turn-off is thus consistent with what the measurements at isothermal conditions gave; no PDs were detected at these temperatures in objects A and B, see Figure 6.

The PDs which started to appear a few minutes into the cooling period are probably a result of that shrinkage voids were formed in the innermost layers of the insulation. The thermal contraction of the mass is here larger and proceeds faster than further out in the insulation, and the electric field is about twice as strong as in the outermost insulation layers.

As discussed earlier, the distinct dissimilarities in the observed PRPD patterns may suggest that a second type of cavities develop as the temperature in the insulation continued to fall. The load cycling breakdowns that have been observed during the type tests usually occur a few hours into the cooling



**Figure 8.** PRPD plot acquired at 70 kV from the cable A. The time lapsed after rated load current turn-off is indicated for each plot. The cable surface temperature was maintained at 6 °C.

period. This is at the same time as the more powerful type of PDs started appearing in the present study. It may thus be speculated that the PDs generated here under modest ac stress, originate in the same type of defect contributing to the load cycling breakdowns seen under high DC stress in the type test.

The fact that the PDs faded out as the cables reach isothermal conditions after having carried load current is unexpected. The combined cavity volume is now at its largest since the average temperature in the insulation is at its lowest. Under isothermal conditions and before cable A had carried any load currents, the inception and extinction voltages at 6 °C were 30 and 8 kV, respectively, see Figure 6a. Now, 1,300 min after a load turn-off on the same cable and at the same temperature, only few PDs were recorded at 70 kV. When reducing the voltage to 40 kV for a second measurement, all PDs had extinguished. Apparently, the dielectric strength of the cavities was here substantially increased by the current loading.

In the tests presented in Section 3.2, the PD behavior of a cable was also significantly altered by passing load currents, see Figure 6c. However, in that case the dielectric strength of the cavities was not increased, but significantly reduced (although it one month later was back to its original level).

### 3.5 MECHANISMS AND TIME CONSTANTS

The mechanisms responsible for the current-induced change in PD behavior have not been identified. As mentioned earlier, a pressure-driven radial flow of mass through the paper, changes in the internal gas pressure of the cavities, their size and number, and other phenomena can play roles in this. Irrespective of the nature of the dominating mechanism(s), two important aspects stand out: First, this may also affect the dielectric strength of the insulation system under HVDC operation. Second, the associated time constants are of the order of days and weeks.

The electric field and thus also the dielectric stresses in the insulation of a HVDC MIND cable are to a large extent determined by the space charge distribution. Under stationary conditions, the radial space charge distribution is determined by the temperature gradient through the insulation. Changes in the current loading alter both the maximum temperature (at the conductor) and the thermal gradient through the insulation. (The temperature of the ambient – sea water or mud – is assumed to be constant over the time spans considered.) Hence, a current load change is followed by a space charge redistribution. Reversing the polarity, which is done regularly on many MIND cables in operation, initiates even greater changes in the space charge distribution.

Consequently, when estimating the dielectric stresses which the insulation of a MIND cable is exposed to during load changes and polarity reversals, both the thermal time constant of the cable and the time constant associated with the space charge redistribution are taken into account. For a typical HVDC MIND cable, the thermal time constant is around half a day, whereas the time needed for the space charges to reach a new equilibrium (and the dielectric stress to come down) may be substantial at low temperatures. At 10 °C ambient it takes approximately a day.

The dielectric stresses associated with frequent polarity reversals and rapid and large load changes are much larger than under steady state conditions, so the ability for MIND cables to

endure this over a lifetime has been questioned. As a precautionary measure, several HVDC links using MIND cables have implemented operational restrictions on the rate of load changes and are also applying certain procedures that ease stresses during polarity reversals.

The results from the present investigation with PD measurements under ac (where no space charge phenomena exist) strongly suggest that current loading alone can change the dielectric properties of the MIND cable insulation. Consequently, accurate determination of the limitations of an HVDC MIND cable with regard to what load changes and polarity reversals it can safely handle, may be more complicated than previously assumed. It may not be sufficient to consider the loading history only from temperature and space charge redistribution perspectives. Mechanisms with an even larger time constant – of the order of days and weeks – may be needed to be included in the considerations.

Obviously, identifying and understanding all the mechanisms at work in the insulation under dynamic conditions would be a good starting point for utilizing the full potential of the MIND cable technology.

## 4 CONCLUSIONS

PD measurements at modest ac voltages is a new and inexpensive approach for studying the insulation system of full-scale MIND HVDC subsea cables.

The observed temperature dependency of the PD activity supports the existing perception that thermal contraction of the mass causes potentially harmful cavities to form in the insulation after a load turn-off and at low temperatures.

The observation of two distinctly different PRPD patterns at different stages in the cooling period after a load turn-off suggests that different "types" of cavities are created. The type causing by far the most powerful PDs appears a few hours into the cooling period, which coincides in time with when load cycling breakdowns during type testing occur.

Current loading leaves the cavities with a different dielectric strength afterwards; both large increases and a temporary reduction were observed. The mechanisms behind are not identified, but the associated time constants are of the order of days and weeks. Considering the market demand for more rapid load changes, fully understanding the dynamic behavior of the insulation system of MIND cables is crucial for exploring the true potential of this technology.

## ACKNOWLEDGMENT

This work was supported in part by the Norwegian Research Council, Statnett, Nexans Norway, National Grid Electricity Transmission, TenneT TSO, Fingrid, and Svenska Kraftnät under contracts no. 208726/E20 and 256505/E20.

## REFERENCES

- [1] T. Worzyk, *Submarine Power Cables: Design, Installation, Repair, Environmental Aspects*, Berlin, Heidelberg, Germany: Springer, 2009.
- [2] A. Eriksson, G. Henning, B. Ekenstierna, U. Axelsson, and M. Akke, "Development work concerning testing procedures of mass-impregnated HVDC cables," *Int. Council Large Electric Systems (CIGRÉ)*, 1994, Paper no. 21-206.

- [3] CIGRÉ Working Group 21-01, "Recommendations for tests of power transmission DC cables for a rated voltage up to 600 kV," *Electra*, no. 72, pp. 105-114, 1980.
- [4] CIGRÉ Working Group 21-02, "Recommendations for tests of power transmission DC cables for a rated voltage up to 800 kV," *Electra*, no. 189, pp. 39-55, 2000.
- [5] P. Gazzana Priaroggia, P. Metra, and G. Miramonti, "Research on the breakdown under type test of non-pressurized paper-insulated HVDC cables," *European Trans. Electric Power*, vol. 3, no. 5, pp. 321-330, 1993.
- [6] G. Evenset and G. Balog, "The breakdown mechanism of HVDC mass-impregnated cables," *Int. Council Large Electric Systems (CIGRÉ)*, 2000, Paper no. 21-303.
- [7] G. Evenset, "Cavitation as a precursor to breakdown of mass-impregnated HVDC cables," PhD dissertation, Norwegian Univ. Science and Technology, Trondheim, Norway, 1999.
- [8] G. Evenset, J. Sletbak, and O. Lillevik, "Cavity formation in mass-impregnated high voltage direct current cable insulation," *Annu. Rep. Conf. Electr. Insul. Dielectr. Phenom. (CEIDP)*, 1998, pp. 554-559.
- [9] P. Szabo, O. Hassager, and E. Strøbech, "Modeling of pressure effects in HVDC cables," *IEEE Trans. Dielectr. Electr. Insul.*, vol. 6, pp. 845-851, 1999.
- [10] M. Runde, R. Hegerberg, N. Magnusson, E. Ildstad, and T. Ytrehus, "Cavity formation in mass-impregnated HVDC subsea cables – Mechanisms and critical parameters," *IEEE Electr. Insul. Mag.*, vol. 30, pp. 22-33, 2014.
- [11] Z. Y. Huang, J. A. Pilgrim, P. L. Lewis, S. G. Swingler, and G. Tzemis, "Thermal-electric rating method for mass-impregnated paper-insulated HVDC cable circuit," *IEEE Trans. Power Del.*, vol. 30, pp. 437-444, 2015.
- [12] Z. Y. Huang, J. A. Pilgrim, P. L. Lewis, S. G. Swingler, and G. Tzemis, "Dielectric thermal-mechanical analysis and constrained high voltage DC cable rating," *IEEE Trans. Dielectr. Electr. Insul.*, vol. 22, pp. 2826-2832, 2015.
- [13] M. J. P. Jeroense and F. H. Kreuger, "Partial discharge measurements on a high voltage direct current mass impregnated paper cable," *IEEE Int. Symp. Electr. Insul. (ISEI)*, 1996, pp. 134-137.
- [14] J. Elovaara, U. Jonsson, G. Henning, and E. Peterson, "PD measurements as a tool in upgrading the transmission capacity of the Fenno-Skan HVDC cable," *Int. Council Large Electric Systems (CIGRÉ)*, 2002, Paper no. 21-302.
- [15] CIGRÉ Working Group D1.33, "High voltage on-site testing with partial discharge measurements," *CIGRÉ Techn. Brochure no. 502*, 2012.
- [16] High voltage Test Techniques – Partial Discharge Measurements, IEC Standard 60270, 2000.
- [17] R. Liao, J. Yan, L. Yang, M. Zhu, and B. Liu, "Study on the relationship between damage of oil-impregnated insulation paper and evolution of phase-resolved partial discharge patterns," *Eur. Trans. El. Power*, vol. 21, pp. 2112-2124, 2011.
- [18] T. Shahsavarian and S. M. Shahrtash, "Modelling of aged cavities for partial discharge in power cable insulation," *IET Sci. Meas. Technol.*, vol. 9, pp. 661-670, 2015.